

Crack tip 90° domain switching in tetragonal lanthanum-modified lead zirconate titanate under an electric field

Fei Fang, Wei Yang, and Ting Zhu

Failure Mechanics Laboratory, Department of Engineering Mechanics, Tsinghua University, Beijing 100084, China

(Received 15 September 1998; accepted 6 April 1999)

Lanthanum-modified lead zirconate titanate ferroelectric ceramics ($\text{Pb}_{0.96}\text{La}_{0.04}\text{(Zr}_{0.40}\text{Ti}_{0.60})_{0.99}\text{O}_3$) were synthesized by the conventional powder processing technique. X-ray diffraction experiments revealed that the samples belong to the tetragonal phase with $a = b = 0.4055$ nm, $c = 0.4109$ nm, and $c/a = 1.013$. After being poled, the samples were indented with a 5-kg Vickers indenter, and lateral electric fields of $0.4 E_c$, $0.5 E_c$, and $0.6 E_c$ ($E_c = 1100$ V/mm) were applied, respectively. Field-emission scanning electron microscopy showed that 90° domain switching appeared near the tip of the indentation crack under a lateral electric field of $0.6 E_c$. A mechanism of 90° domain switching near the crack tip under an electric field is discussed.

I. INTRODUCTION

Perovskite-type ferroelectric ceramics have been used as sensors, actuators, and transducers in smart structures. Their properties can be tailored by changing compositions and processing conditions. However, ferroelectric ceramics are brittle and they may degrade under combined electrical and mechanical fields. The lack of reliability limits the performance of ferroelectric devices and raises the need to understand electrical fracture and toughening mechanisms of ferroelectric ceramics. Vickers indentation experiments indicate that the fracture toughness of poled ferroelectrics is anisotropic. Upon indentation, the crack propagating along the poling direction has a shorter length and, consequently, an apparently higher fracture toughness; the crack propagating normal to the poling direction has a longer length and an apparently lower fracture toughness.¹⁻³ Three-point bending and compact-tension tests on the poled lead zirconate titanate (PZT) ceramics demonstrated that, for cracks perpendicular to the poling axis, a field applied in the poling direction promoted the cracking, whereas a field antiparallel to the poling direction inhibited cracking.⁴

The microstructure of ferroelectric ceramics is characterized by ferroelectric domains with different orientations. They may undergo polarization switches under electrical or mechanical fields. Theoretical analyses⁵⁻⁷ and an x-ray diffraction (XRD) experiment⁸ indicated that 90° domain switching plays an important role in the fracture and fatigue behavior of ferroelectric ceramics. Yang and Zhu⁵ proposed a model of stress-assisted 90°

degree polarization switch to quantify the toughening process. By assuming a uniform electric field, they provided a plausible explanation for the fracture toughness anisotropy and for the asymmetry of fracture toughness under a positive and a negative electric field. Zhu and Yang⁶ extended the model to the case of a concentrated electric field near the crack tip. Fulton and Gao⁷ studied the electrical nonlinearity in the fracture of ferroelectric ceramics based on a Dugdale type assumption that the domain switching zone near the crack tip takes a strip shape. By using XRD techniques, Mehta and Virkar⁸ verified the existence of 90° domain switching in the fractured surface of a single edge notched beam sample broken in four-point bending at room temperature. Fan *et al.*⁹ revealed the residual domain switching in a transparent relaxor-type ferroelectric 9.4/65/35 lanthanum-modified lead zirconate titanate (PLZT) under a mechanical stress field with an optical microscope. However, direct observation of the 90° domain switching zone near a crack tip for tetragonal ferroelectric ceramics under an electric field has yet to be revealed experimentally.

In this paper, PLZT ferroelectric ceramics ($\text{Pb}_{0.96}\text{La}_{0.04}\text{(Zr}_{0.40}\text{Ti}_{0.60})_{0.99}\text{O}_3$) were synthesized by a conventional powder processing technique. XRD was used to reveal the lattice structure. After being polished, poled, and indented by a 5-kg indenter, lateral electric fields of 0.4, 0.5, and $0.6 E_c$ ($E_c = 1100$ V/mm) were applied. Scanning electron microscopy (SEM) studies on the etched surfaces of unpoled and poled PLZT specimens, as well as the poled specimens with indentation cracks under different lateral electric fields, were carried out. The 90°

domain switching was revealed on the etched surfaces in the $(\text{Pb}_{0.96}\text{La}_{0.04})(\text{Zr}_{0.40}\text{Ti}_{0.60})_{0.99}\text{O}_3$ sample under a lateral electric field of $0.6 E_c$. The observed 90° domain switching is attributed to the intense electric field near the crack tip. The mechanism for the crack tip 90° domain switching is discussed.

II. EXPERIMENTAL PROCEDURE

$(\text{Pb}_{0.96}\text{La}_{0.04})(\text{Zr}_{0.40}\text{Ti}_{0.60})_{0.99}\text{O}_3$ (PLZT) ceramics were synthesized by the conventional powder processing technique. High-purity powders of Pb_3O_4 , ZrO_2 , La_2O_3 , and TiO_2 were properly weighed and mixed by ball milling in alcohol. After they were dried and sieved, the powders were calcined in a closed alumina crucible at 800 °C for 1 h. After calcining, the powders were remilled, dried, sieved, and then pressed into a rectangular shape and sintered in a closed alumina crucible at 1200 °C for 2 h; then they were furnace cooled to room temperature. During sintering, the PbO atmosphere was maintained by pellets of PbZrO_3 with 1 to 2 wt% excess of PbO. The lattice structure of the PLZT sample was analyzed with a D/max-III B x-ray diffractometer using Cu K_α radiation.

The PLZT ceramic samples were then mechanically cut and ground into specimens ($3.5 \times 5 \times 25$ mm). One 5×25 mm surface was ground and polished. The two opposing 5×25 mm surfaces were sprayed with Au electrodes. The samples were then poled under an electric field of 8 kV over a width of 3.5 mm at 120 °C. After the Au electrodes were removed, the polished surface of 5×25 mm was indented under a 5-kg load. Then, the two opposing surfaces of 3.5×25 mm were sprayed with Au electrodes and lateral electric fields of 0.4, 0.5, and $0.6 E_c$ were applied. Figure 1 illustrates the specimen configuration, the poling direction, the indentation induced surface cracks, and the direction of the lateral electric field. Later, unpoled, poled, and poled PLZT ceramics with different lateral electric fields were etched by using a solution made up of the following mixture: 2.5 cm^3 of HCl, 47.5 cm^3 of H_2O , and two drops of concentrated

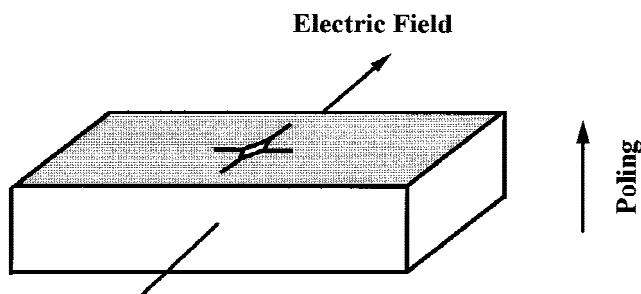


FIG. 1. Illustration of specimen configuration, poling direction, indentation-induced surface cracks, and direction of the lateral electric field.

HF. The samples were then cleaned ultrasonically in ethanol and examined in a JSM-6301F field-emission SEM.

III. RESULTS AND DISCUSSION

Figure 2 is the XRD pattern of $(\text{Pb}_{0.96}\text{La}_{0.04})(\text{Zr}_{0.40}\text{Ti}_{0.60})_{0.99}\text{O}_3$ ceramics. It reveals that, at room temperature, PLZT ceramics adopt a tetragonal perovskite structure with $a = b = 0.4055$ nm, and $c = 0.4109$ nm. Consequently, the aspect ratio c/a is 1.013. A SEM fractograph of the fracture surface for PLZT ceramics is shown in Fig. 3, which indicates that the synthesized PLZT ceramics is fully densified with a well-formed grain structure. PLZT ceramics with tetragonal structure are ferroelectric, with the direction of spontaneous polarization parallel to the elongated c axis. If the c axis of the domain is parallel-normal to the viewing direction, it is termed a c -type- a -type domain. There are four types of domain boundaries in a tetragonal ferroelectric phase: (1) 90° a - a boundaries, (2) 90° a - c boundaries, (3) 180° a - a boundaries, and (4) 180° c - c boundaries.

The etching rates of ferroelectric domains with different orientations are different: the positive ends of the domain etch at the highest rate, the negative ends of the domains etch at the lowest rate, and the domains whose polarization vectors are parallel to the surface etch at an intermediate rate. Thus, the c^- domains appear bright, c^+ domains appear dark, and the a domains appear gray in a SEM micrograph.¹⁰ For unpoled PLZT ceramics, the SEM morphology in Fig. 4(a) is dominated by lamellar strips because of the 90° changes in the polar direction. The 180° domain boundary is also observed in the micrograph. To minimize the charge at the domain wall, the polarization vectors in a ferroelectric phase usually adopt a head-to-tail arrangement across the 90° boundary. A schematic illustration of the M region in Fig. 4(a) is shown in Fig. 4(b).

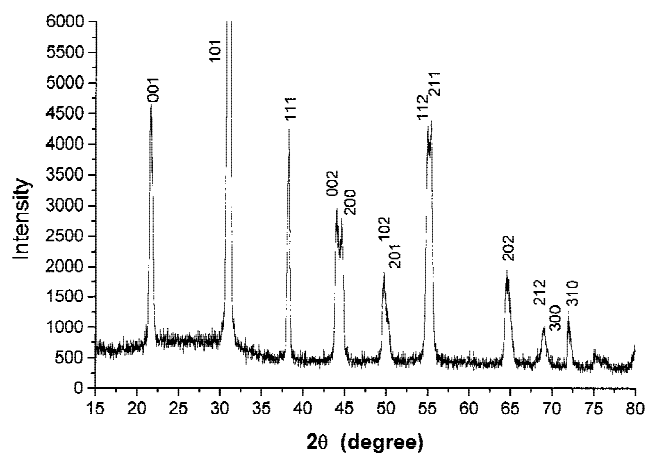


FIG. 2. XRD pattern of PLZT ceramics.

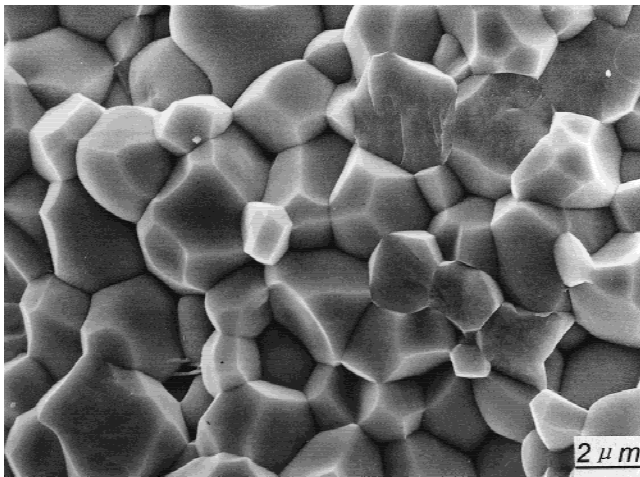
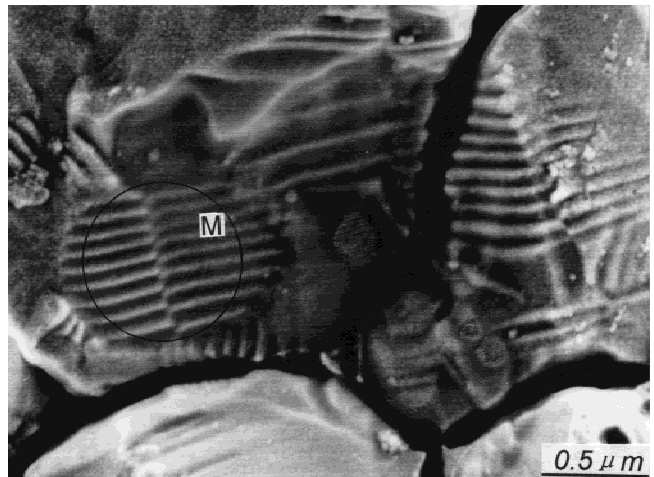
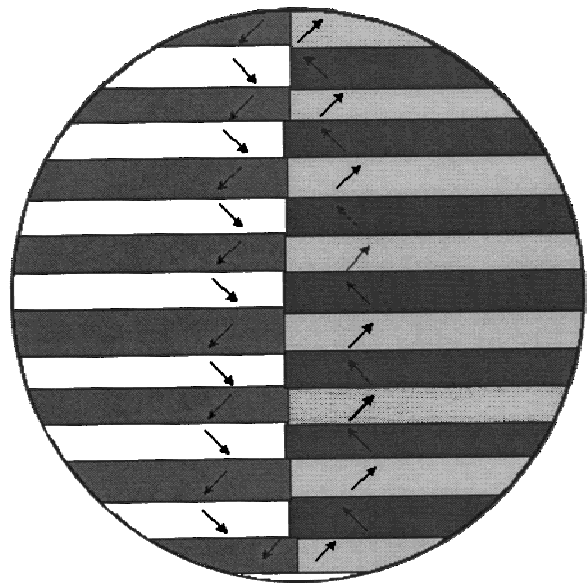


FIG. 3. SEM fractograph of PLZT ceramics.



(a)

Polycrystalline ceramics that have not been subjected to a static field would behave as a nonpolar material. However, by applying a static field, ferroelectric ceramics can be transformed into polar material through the process of 90° and 180° domain switchings. A switch of 180° causes little strain and is activated by the electric field. On the other hand, switching of 90° can be produced by electric or stress fields. It delivers a sizeable strain of fixed amount and orientation, contracting along the previous polarization direction and elongating along the current one. When the electric field is removed, residual elongation and polarization remain. The poling process of ferroelectric ceramics is illustrated in Fig. 5. Overall observation of the poled PLZT ceramics under SEM indicated that there are no parallel lines of 90° changes in the polar direction, as shown in Fig. 6. However, topographic contrasts are still visible among different crystallites, which are due to the random orientations of the crystallographic axes of the crystallites.



(b)

FIG. 4. (a) SEM morphology of the etched surface for unpoled PLZT ceramics. (b) Schematic illustration of the M region.

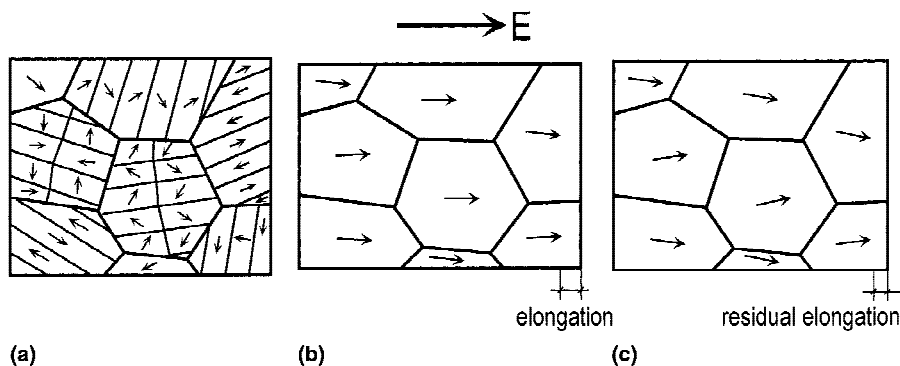


FIG. 5. Poling process of ferroelectric ceramics: (a) domain structure before poling, (b) domain structure and elongation under a poling electric field, and (c) domain structure and residual elongation after poling.

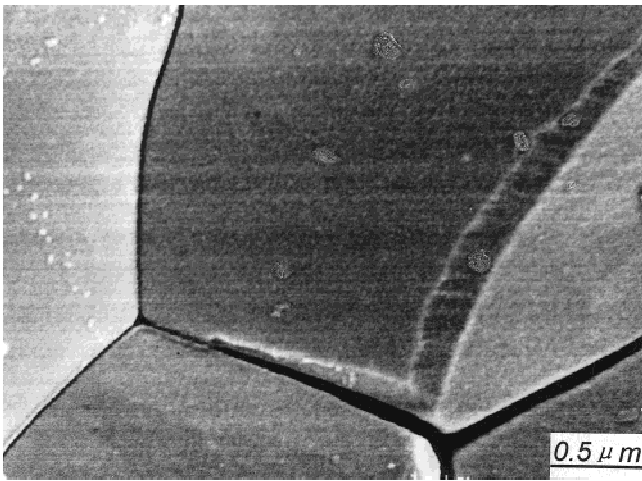


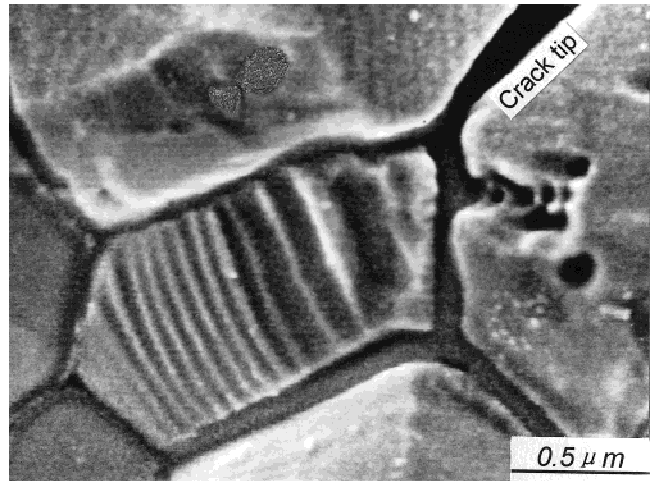
FIG. 6. SEM morphology of the etched surface for poled PLZT ceramics.

After the poled PLZT ceramic samples are indented by a 5-kg load and then subjected to different lateral electric fields, their domain structures near the indentation cracks may change. The crack tip domain switching zone was observed by SEM. It was shown that in poled PLZT with $0.6 E_c$ lateral electric field, lamellar 90° domain structure reappeared, illustrating the formation of 90° domain switching near the crack tip, as shown in Fig. 7(a).

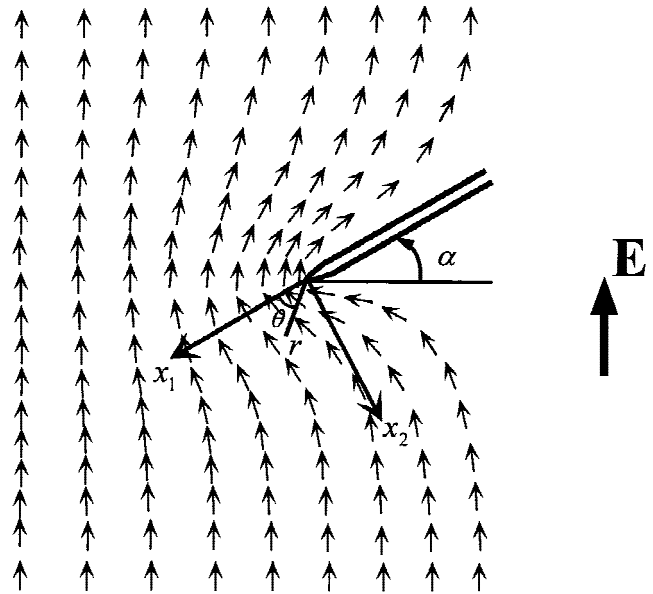
Similar to any solid-phase transformation, 90° domain switching is driven by the reduction of free energy. As shown in Fig. 7(b), the indentation crack forms an inclination angle α with the horizontal axis. The remotely applied electric field \mathbf{E} directs upward. Denote the electric field distribution within the specimen by two components, E_1 and E_2 , along the local coordinates x_1 (tangential to the crack) and x_2 (normal to the crack), respectively. The applied electric field can be decomposed into a component of $E \sin \alpha$ parallel to the indentation crack and a component of $E \cos \alpha$ normal to it. The former causes only uniform field distribution within the specimen, but the latter causes field concentration near an impermeable crack. The electric field concentration near the indentation cracks provides a much larger driving force for 90° domain switching. The singular part of the crack tip electrical field can be described by^{6,11}

$$\begin{Bmatrix} E_1 \\ E_2 \end{Bmatrix} \approx \frac{K_E}{\sqrt{2\pi r}} \begin{Bmatrix} -\sin(\theta/2) \\ \cos(\theta/2) \end{Bmatrix} \quad (1)$$

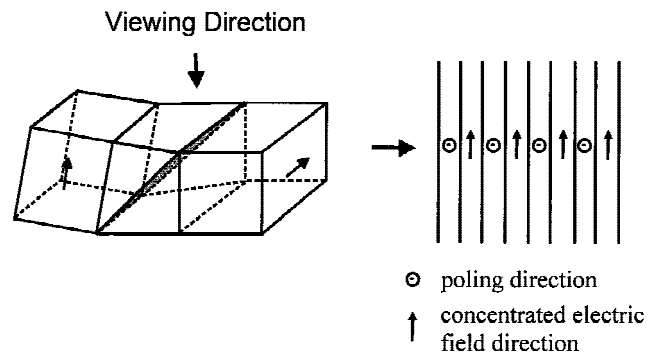
where r and θ are polar coordinates centered at the crack tip. K_E measures the intensity of the crack tip electrical field and is given by $E \cos \alpha \sqrt{\pi l}$, where l denotes the half length of the insulated crack. Directly ahead of the crack tip, the field concentration is intense and aligned normal to the crack extension line, as depicted in Fig. 7(b). For the experimental conditions we used, it was always perpendicular to the poling direction. Conse-



(a)



(b)



(c)

FIG. 7. (a) SEM morphology of the etched surface for poled PLZT ceramics with $0.6 E_c$ lateral electric field, showing 90° domain switching zone near a crack tip, (b) concentrated electric field near a crack tip, and (c) schematic illustration of the unconventional a-c domain boundary.

quently, 90° domain switching takes place in several strips in the grain ahead of the crack tip, leading to marks of straight 90° domain walls. Schematic representation of the a–c domain boundary in the domain switching zone of Fig. 7(a) is shown in Fig. 7(c). This kind of ferroelectric domain boundary was found in doped BaTiO₃ ceramics and was termed the unconventional domain boundary.¹⁰ Compared with the conventional a–c domain boundary, the unconventional domain boundary has higher energy because it has a higher degree of distortion, and there is a net charge at the boundary because of the nature of this domain configuration.¹⁰ However, the concentrated electric field near the crack tip favors the formation of this unconventional domain boundary. Furthermore, the configuration and size of the domain switching zone are influenced by the crack tip field and the constraint of the neighboring grains. Further investigation will be pursued for the influence of the dopant type and concentration on the configuration and size of the domain switching zone and their effect on electrical fracture and fatigue behavior.

IV. CONCLUSIONS

(1) XRD experiments reveal that the synthesized (Pb_{0.96}La_{0.04})(Zr_{0.40}Ti_{0.60})_{0.99}O₃ ceramic sample belongs to the tetragonal phase with $a = b = 0.4055$ nm, $c = 0.4109$ nm, $c/a = 1.013$.

(2) A SEM study on the etched surface of unpoled and poled PLZT ceramics demonstrated that there are lamellar 90° domain structure and 180° domain boundaries in unpoled PLZT but no lamellar 90° domain structure in poled PLZT ceramics.

(3) By applying a 0.6 E_c lateral electric field, 90° domain switching appeared in front of the indentation crack tip. The configuration and size of the 90° domain switching zone are influenced by the crack tip field and the constraint of the neighboring grains.

ACKNOWLEDGMENTS

The authors wish to thank Prof. X.W. Zhang in the Department of Materials Science and Engineering of Tsinghua University for his helpful discussions. The authors also thank the National Science Foundation of China for support of this research project.

REFERENCES

1. A.G. Tobin and Y.E. Pak, in *Smart Structures and Materials 1993: Smart Materials*, edited by V.K. Varadan (Proc. SPIE, **1916**, Albuquerque, NM, 1993) p. 78.
2. R.N. Singh and H. Wang, *Proc. AMD-Vol. 206/MD-Vol. 58 Adaptive Materials Systems*, edited by G.P. Carman, C. Lynch, and N.R. Sottos (ASME, New York, 1995), p. 85.
3. C.S. Lynch, *Acta Mater.* **46**, 599 (1998).
4. S. Park and C.T. Sun, *J. Am. Ceram. Soc.* **68**, 259 (1995).
5. W. Yang and T. Zhu, *J. Mech. Phys. Solids.* **46**, 291 (1998).
6. T. Zhu and W. Yang, *Acta Mater.* **45**, 4695 (1997).
7. C.C. Fulton and H. Gao, *Appl. Mech. Rev.* **50**, s56 (1997).
8. K. Mehta and A.V. Virkar, *J. Am. Ceram. Soc.* **73**, 567 (1990).
9. J. Fan, H. Niu, and C.S. Lynch, *J. Mater. Sci. Lett.* **17**, 189 (1998).
10. H.H. Yung, H.M. Chan, X.W. Zhang, and M.P. Harmer, *J. Am. Ceram. Soc.* **69**, 594 (1986).
11. W. Yang and T. Zhu, *Fatigue Fract. Eng. Mater. Struct.* **21**, 1361 (1998).